Design, Test and Fabrication of a Droplet based Microfluidic Device for Clinical Diagnostics

F. Jacinto, A. S. Moita and A. L. N. Moreira
IN+ - Center for Innovation, Technology and Policy Research, Instituto Superior Técnico, Universidade de Lisboa, Av. Rovisco Pais, 1049-001, Lisboa, Portugal

Keywords: Lab-on-a-chip, Droplet based Microfluidics, Clinical Diagnostics, Chip Design and Test, Experimental and Numerical Approaches.

Abstract: Despite the intensive research performed towards the development of biomicrofuidic devices, information on the design, test and microfabrication of the devices is scarcely reported. Following our previous work, this paper describes the design, microfabrication and test of an electrowetting chip to transport and manipulate biosamples, towards the development of a microfluidic device for cancer diagnostics. As a first approach, experiments are performed to infer on the basic chip dimensions and configuration (size and positioning of the electrodes), allowing its best performance, evaluated based on droplet dynamics (spreading/receding diameter and contact line velocity). Then, to scale down this section, for its proper integration in the device, these basic dimensions are introduced as first guess values in a numerical model, used to optimize the distance between the electrodes, the thickness of the dielectric and the electric potential and frequency to be applied.

1 INTRODUCTION

Since their introduction by Manz (1990), lab-on-a-chip devices have shown a fast evolution, based on intensive research. Many applications mainly deal with DNA manipulation and with basic biochemical analysis (e.g. Wheeler *et al.*, 2004) and only recent studies have seriously focused on the development of microfluidic devices for clinical diagnostics (e.g. Dance, 2017).

The most popular configuration in lab-on-chip design is based on the continuous transport of the samples in an immiscible fluid, which flows inside microchannels. Dance *et al.* (2.17) detail the development of microchips capable of performing blood samples separation, isolation of specific cells for further analysis, diagnostics based, for instance, on DNA analysis and cell sorting. These devices, which are mostly focused on cancer diagnostics, are nevertheless all based on microchannel flows. Despite being effective, this configuration addresses several issues related to clogging and maintenance difficulties, lack of flexibility in the design and the requirement of auxiliaries such as pumps and valves, which have a very low efficiency at the microscale (Geng *et al.*, 2017). On the other hand, droplet based digital microfluidics, in which the samples are transported in microdroplets manipulated by electrowetting, is an alternative which may solve many of the limitations of the configuration based on microchannels. In this context, closed configuration systems, where droplets travel between parallel plates are still most often used for sample manipulation and for clinical diagnostics. However, open configuration electrowetting systems, in which the electrodes and counter electrodes are gathered in a single plate over which the droplet is transported, can fully take advantage of the aforementioned positive characteristics of digital microfluidics, but have still several technical difficulties to overcome. The most adequate electrodes configuration depends on the wetting properties of the dielectric material covering the electrodes and on the particular wetting and physico-chemical properties of the samples (e.g. Moita *et al.*, 2016, Geng *et al.*, 2017, Vieira *et al.*, 2017). Furthermore, the affinity of the dielectrics with the biosamples, e.g. proteins, has been reported to locally alter the wettability at the droplet-dielectric surface interface, thus affecting the effectiveness of droplet transport (e.g. Yoon and Garrell, 2003, Moita *et al.*, 2016).

Jacinto, F., Moita, A. and Moreira, A.
Design, Test and Fabrication of a Droplet based Microfluidic Device for Clinical Diagnostics.
DOI: 10.5220/0006656600880095
In *Proceedings of the 11th International Joint Conference on Biomedical Engineering Systems and Technologies (BIOSTEC 2018) - Volume 1: BIODEVICES*, pages 88-95
ISBN: 978-989-758-277-6

Finally, there are numerous papers concerning EWOD – Electrowetting on Dielectric applications on microchips (including lab-on-chip systems), which describe quite well the physics governing electrowetting (from experimental evidence to models), as recently reviewed for instance in Nelson *et al.* (2012), but most of these papers are focused on the fundamentals explaining droplet motion, rather than on device fabrication. Relating the fundamentals with device fabrication, however is not always easy and erroneous relations may ultimately preclude the development of an efficient device, as explained for instance by Li *et al.* (2012).

Within this scope, the present paper addresses the design and test of a simple lab-on-chip configuration, towards the development of a microfluidic device applied for cancer diagnostics, based on cells elasto-mechanical properties and on the particular rheology of the fluid droplets transporting the biosamples. These properties are then expected to be correlated with the different stages of cell stiffness, which in turn be used for cancer diagnostics, following the work of for instance Gosset *et al.* (2010). Hence succeeding previous work (Vieira *et al.*, 2017), which introduced the microfluidic device, as a whole and focused on the effects of the properties of the dielectrics and of the biosamples, this paper addresses the configuration of the transport section of this device, namely on the dimensions and positioning of the electrodes. First, an experimental approach is followed to infer on the basic dimensions, allowing the best performance, evaluated based on droplet dynamics (spreading/receding diameter and contact line velocity). Then, to scale down this section for a proper integration in the device, these basic dimensions are introduced in a numerical model, used to optimize the distance between the electrodes, the thickness of the dielectric and the electric potential and frequency to be applied. The main difficulty and novelty in this device is the proper manipulation and transport of the droplets using the dynamic behaviour and its relation with the physico-chemical properties of the fluids for the diagnostics. In the current stage of development, droplet dynamics (contact diameters and angles) is used to optimize the configuration of the chip namely the size and position of the electrodes. Despite looking a basic task, it is usually performed on a trial-and-error basis, not considering droplet dynamics. In this work, given that droplet dynamics, related to the fluids rheology is useful for the diagnostics itself, using the parameters describing droplet dynamics (spreading diameter, spreading velocity and contact angles) to optimize the size and position of the electrodes is a relevant approach, as the chip is configured, from the start, as a function of the parameters useful for the diagnostics.

2 MANUSCRIPT PREPARATION

2.1 Experimental Method

Test chips, microfabricated at INESC-MN (Institute for Systems Engineering and Computers – Microsystems and Nanotechnologies) are composed by arrays of interdigited electrodes printed on a 0.6 μm aluminium film by lithography and wet etch on a glass substrate with 102x45 mm^2 and 700 μm width. A thin film of a dielectric material (PDMS – Polydimethylsiloxane) was deposited on the chip assembly, without covering the contacts. The different configurations tested only vary in the electrodes width, w ($120 \leq w \leq 1400$ μm), being the numerous interdigitated coplanar electrodes displaced with a fixed distance between them, $2a$=60 μm. The chips are actuated using DC current provided by a Sorensen DCR600-.75B power supply. The applied voltage was varied from 0 to 245 V. The frequency imposed for switching the polarities at the electrodes is programmed using a square wave, as in Fan *et al.* (2007). The imposed frequencies were varied between 0 and 400Hz.

The performance of the chips is evaluated looking at the dynamic response of the droplets on the chips, which in turn is discussed based on the measurement of several quantities such as the spreading diameter (diameter of the droplet as it spreads on the surface), the contact angles under actuation and the velocity of the contact line (derivative of the spreading diameter). These quantities are determined from high-speed visualization and post-processing. The high-speed images are taken at 2200 fps using a Phantom v4.2 from Vision Research Inc., with 512x512 pixels@2100fps resolution. For the present optical configuration, the spatial resolution is 25μm/pixel and the temporal resolution is 0.45 ms. The post-processing is performed using a home-made routine developed in Matlab. Temporal evolution of the contact (spreading and receding) diameters is presented as the average curve of at least 6 events (6 droplets), obtained under similar experimental conditions. Each curve depicting the temporal evolution of the spreading diameters requires nearly 500 measurements. So, 6 complete curves are

considered for each voltage, frequency, electrode configuration, i.e. for all the parameters varied in the study. Then, maximum/averaged vales are taken to obtain the discrete values for the velocity and for D/D_0. Contact angle measurements are averaged from twelve events.

All the experiments were performed in a Perspex chamber, saturated with the working fluid and the tests were performed under continuous monitoring of temperature and relative humidity of the surrounding air. The measurements were taken with a DHT 22 Humidity & Temperature Sensor, at a sample rate of 0.5 Hz. Relative humidity was measured within 2-5% accuracy, while temperature measurements were taken within ±0.5°C accuracy. The temperature was observed to be constant within T=20±3ºC and relative humidity was kept constant between 75% and 78%.

Detailed description of the experimental method and procedures used can be found in Moita *et al.* (2016) and in Vieira *et al.* (2017).

The biofluid used here is a solution of GFP – Green Fluorescent Protein, (produced and purified in house) with $1.71x10^{-3}$ mM concentration. The solution was characterized in terms of density, surface tension and viscosity, as summarized in Table 1 and following the procedures described in Moita *et al.* (2016) and in Vieira *et al.* (2017). The GFP solution depicted a Newtonian behaviour, from the rheological point of view. The volume of the produced droplets is set between 1.5 and 2μL.

Table 1: Physico-chemical properties of the GFP solution used in the present work.

Solution	Density ρ [kg/m^3]	Surface tension σ_{lv} [mN/m]	Dynamic viscosity μ [Ns/m^2]
GFP ($1.71x10^{-3}$ mM)	998	72.2±0.7	$1x10^{-3}$

2.2 Numerical Method

The simulations were performed using COMSOL Multiphysics 4.3b. To evaluate the electric forces generated, the numerical domain considered was a 0.655mm radius sphere (droplet domain) within an air space of 3.21x1.6x3mm^3. The electrostatic boundary conditions are an electrical potential of 70V imposed to the electrode on the right (positive x-axis) and a ground (0V) imposed the electrode on the left (Fan *et al.*, 2007). The model considers a thin low permittivity gap with a 10μm dielectric layer (Mata *et al.*, 2016). The mesh is composed of 67025 tetrahedral elements, being refined at the liquid-solid and liquid-vapor interfaces.

For the simulation of droplet motion under transient conditions, the electrostatic boundary conditions are similar, but the distance between electrodes is imposed as $2a$ = 10μm, following the analysis of the electric force, as a function of this distance (as later discussed in the results). The numerical domain is a 0.655mm radius sphere (droplet domain) within an air space of 5X2mm^2. The mesh in this case is composed of 35831 free triangular elements, being also refined at the liquid-surface and liquid-air interfaces.

The electrostatic force actuating on the droplet is calculated using the Maxwell stress tensor, integrated on the droplet surface. A global evaluation method was used to perform this integral in COMSOL. Hence, the electrostatic force is calculated by integrating:

$$n_1 T_2 = -\frac{1}{2} n_1 (E.D) + (n_1.E) D^T \quad (1)$$

on the surface of the droplet, where E is the electric field, D the electric displacement, and n_1 the outward normal from the object. Using the Maxwell stress tensor for a 2D configuration, the volume force is calculated as the first derivative of this tensor.

Regarding the droplet flow, Phase Field User Interface is used to track the liquid-air interface, for a laminar flow, using the incompressible formulation of the Navier-Stokes equations:

$$\rho \frac{\partial u}{\partial t} + \rho\,(u.\nabla) = \nabla.[-\mathrm{pI} + \mu(\nabla \mathrm{u} + \nabla u^T)] + F_g + F_g + F_{ext} + F \quad (2)$$

$$\nabla.\mathrm{u} = 0 \quad (3)$$

The four forces on the right-hand side of eq. (2) are due to gravity, surface tension, external contribution to the free energy, and a user defined volume force.

The phase field method adds the following equations:

$$\frac{\partial \Phi}{\partial t} + u.\nabla\Phi = \nabla.\frac{\gamma\lambda}{\varepsilon^2}\nabla\psi \quad (4)$$

$$\psi = -\nabla.\varepsilon^2\nabla\Phi + (\Phi^2 - 1)\Phi + (\frac{\varepsilon^2}{\lambda})\frac{\partial f_{ext}}{\partial \Phi} \quad (5)$$

where the quantity λ (SI unit: N) is the mixing energy density and ε (SI unit: m) is a capillary width that scales with the thickness of the interface. These

two parameters are related to the surface tension coefficient, σ (SI unit: N/m), through equation:

$$\sigma = \frac{2\sqrt{2}}{3}\frac{\lambda}{\sigma} \quad (6)$$

The volume fraction of air (fluid 2) is computed as:

$$V_f = \min(\max([1+f)/2],0,1) \quad (7)$$

where the min and max operators are used so that the volume fraction has a lower limit of 0 and an upper limit of 1. The density is then computed by:

$$\rho = \rho_1 + (\rho_2 - \rho_1)V_f \quad (8)$$

and the dynamic viscosity according to

$$\mu = \mu_1 + (\mu_2 - \mu_1)V_f \quad (9)$$

where ρ_1 and ρ_2 are the densities and μ_1 and μ_2 are the dynamic viscosities of fluid 1 (biofluids) and fluid 2 (air), respectively.

3 RESULTS AND DISCUSSION

As aforementioned in the Introduction, the entire microfluidic device under development has three main sections: the transport section, the diagnostics section and the sorting section. This paper will focus on the configuration of the first, given the paramount role of an effective transport and manipulation of the samples in the entire device. The motion of the droplet requires it to be in contact with at least two electrodes, which are actuated according to an imposed switching frequency. The imposed duty cycle, which acts as the switching frequency between electrodes, was programmed to vary between 0Hz and 400Hz, so one can infer on the effect of this frequency on the dynamic response of the droplet. Following the recommendations of Chen *et al.* (2004) to evaluate the chip capacitance, the distance between electrodes *a* should be much smaller than their width *w*. So, after some preliminary calculations, four basic configurations were tested, namely, *w* = 120μm, 800 μm, 1200 μm and 1400 μm, with a fixed distance between electrodes, 2*a* = 60μm.

The chips performance is evaluated based on the dynamic response of the droplets under actuation, namely evaluating the spreading diameter, made non-dimensional with the initial diameter of the deposited droplet, the contact angles measured under actuation and the velocity of the contact line. It is worth reminding that the droplets are formed from the solution of GFP ($1.71x10^{-3}$mM). The main objective is to set the width and distance between the electrodes which maximizes droplet spreading diameter and velocity for various conditions of imposed frequency and imposed voltage. The later should be as low as possible to avoid dielectric breakdown.

Figure 1 shows the contact angle obtained under electrostatic actuation, as a function of the applied electric potential, for different imposed frequencies and the temporal evolution of the spreading contact diameter of a droplet on two coplanar electrodes, with *w*=1400 μm, for 350 Hz, with different values of the applied electric potential. Consistently with the Young-Lippmann equation, the contact angle decreases with the increment of applied tension and, consequently, the spreading droplet diameter is larger for increasing imposed voltages for the same frequency, being this trend observed, regardless of the configuration set-up.

The trend observed for the contact angles is in line with the results expected, at the light of Young-Lippmann equation and evidences the independence of the contact angles with the imposed frequency. This indicates that the spreading diameter is independent from the imposed frequency which can be lowered, to simplify the chip arrangement and programming.

Figure 2 emphasizes that the droplet motion is irreversible due to the high adhesion force of the PDMS substrate. Hence after the spreading of the droplet, up to its maximum diameter, this strong adhesion due to the high contact angle hysteresis (larger than 20º, as reported in previous work – Vieira *et al.*, 2017) promotes energy dissipation at the contact line, thus restraining the spreading motion of the droplet. The energy dissipation during this motion precludes the recoiling, thus turning the motion of the droplet irreversible. Consequently, it is difficult for the droplet to be transported to the subsequent electrodes. The dynamic behaviour of the droplet illustrated here for 230 V, is consistently observed for all the applied voltages, in steps of 15 V between 200 and 245 V.

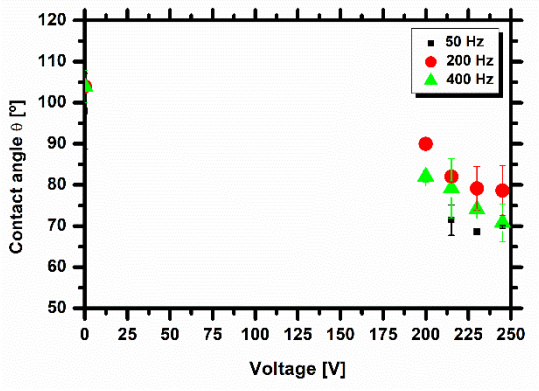

(a)

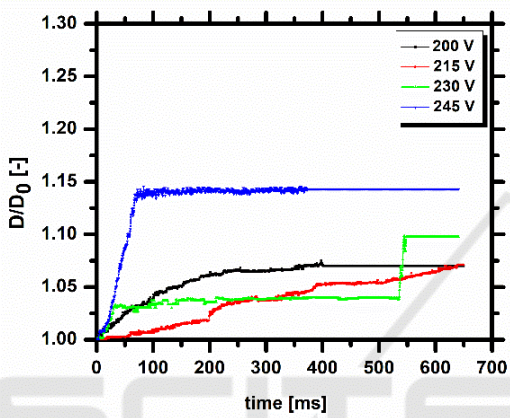

/(b)

Figure 1: (a) Contact angle as a function of the applied electric potential for different imposed frequencies and (b) evolution of the spreading diameter for 350 Hz of a GFP droplet, for the configuration $2a$=60 μm and w=1400 μm. The dielectric substrate is PDMS. The volume of the liquid droplet is 1.8μL.

In a more quantitative approach, the spreading velocity and the maximum diameter of the droplet, as a function of the imposed frequency are shown in figure 2, for the different voltages. The current configuration requires very high imposed voltages (above 200 V), being limited to 245 V, as above this value, the dielectric breakdown occurs leading to electrolysis inside the droplet, which in turn generates a violent droplet disintegration, in agreement with the observations reported, for instance by Mugele and Baret (2005) and by Cooney *et al.* (2006). The difference between the green (230 V) and the blue (245 V) lines is small, which may be indicative of contact angle saturation. On the other hand, the minimum voltage required to observe any droplet response to the actuation on the chips is 200 V.

Analysis of figures 2 and 3 suggests that droplet dynamics is nearly independent from the imposed frequency. However, the results suggest that the droplet has a weaker response to low frequencies (50 Hz) and a swifter response for frequencies between 100-300 Hz, although one cannot identify any monotonic trend between the frequency and the spreading diameter or the velocity. On the other hand, maximum spreading diameters are observed for the highest imposed frequency (400 Hz), but the droplet depicts a lower response in time. This trend is attributed to the imposed electric force that must overcome the resistance to droplet motion associated to the energy dissipation on the surface. The velocities obtained here are lower than those reported in other studies in the literature (e.g. Cooney *et al.* 2006, Fan *et al.* 2007, Sen and Kim, 2009), as the chips configuration is not optimized yet. Also, most of the fluids used in the aforementioned studies are salt solutions and not biofluids.

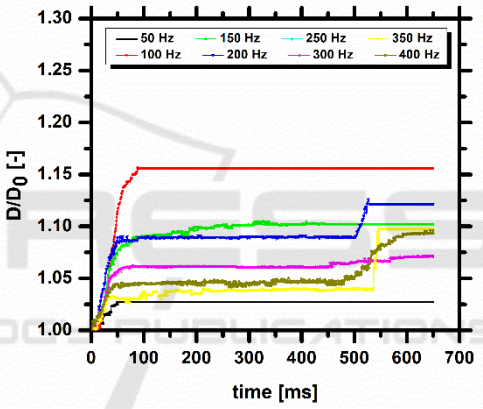

Figure 2: Temporal evolution of the spreading diameter of a GFP droplet on a PDMS substrate, actuated at 230 V for different imposed frequencies, for the configuration $2a$=60 μm and w=1400 μm. The volume of the liquid droplet is 1.8μL.

To infer on the influence of the electrodes width on the dynamic response of the droplets, four alternative electrode configurations were tested. Comparative results between the different configurations are presented in figure 4, which depicts the contact line velocity and the maximum spreading diameter, as a function of the imposed frequency. The results highlight that the configuration with w=120 μm provides the worst droplet response to the electrostatic actuation, expressed by the low values of the spreading velocity and of the non-dimensional spreading diameter D/D_0. The response of the droplet under actuation on all the other configurations is very similar, being however, overall more regular for the

chip with w =1200µm, mainly regarding the values achieved for the maximum diameter.

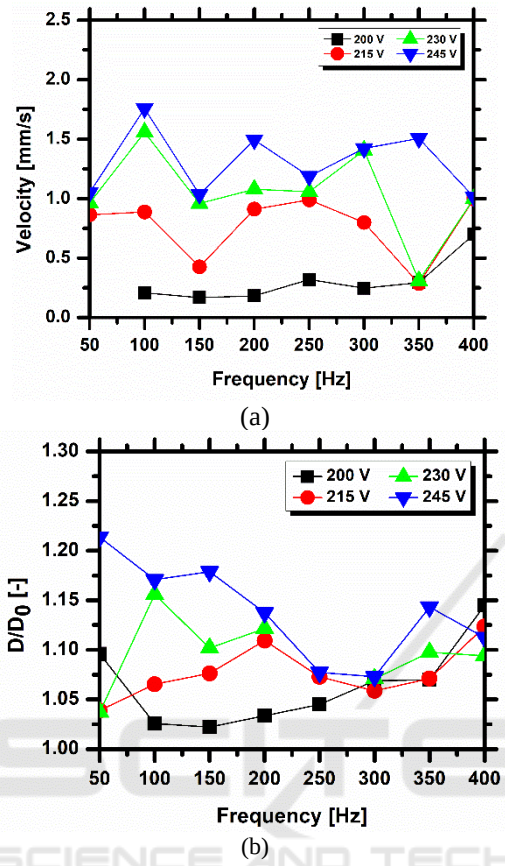

Figure 3: (a) Spreading velocity of the contact line and (b) maximum spreading dimensionless diameter of a GFP droplet on PDMS, moving between coplanar electrodes for the configuration $2a$=60 µm and w=1400 µm for different applied voltages and an imposed frequency. The volume of the liquid droplet is 1.8µL.

In agreement with figures 1 and 2, the set of plots shown here does not identify a monotonic trend between the spreading velocity and diameter and the imposed frequency. Overall it mainly indicates a slower response for very low frequencies (50Hz) and faster response (with larger spreading diameters) for higher imposed frequencies. Nevertheless these plots show that regardless of the imposed frequencies, the configurations with w =1200µm and w =1400µm provide a better dynamic response which enables droplet motion.

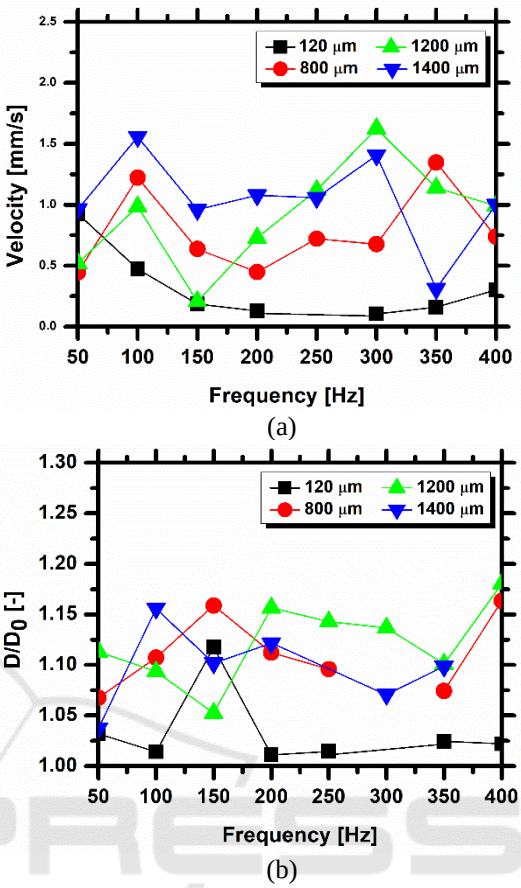

Figure 4: (a) Spreading velocity and (b) maximum spreading dimensionless diameter of a GFP droplet on PDMS, moving between coplanar electrodes for the different configurations, for an imposed frequency of 350Hz and an imposed electric potential of 230 V. The volume of the liquid droplet is 1.8µL.

For all the configurations tested and discussed in the previous paragraphs, the dielectric material used was PDMS, with a thickness of 30µm. This thickness was set following the values reported in the literature and due to some limitations of the microfabrication method, which did not allow a deposition of a thinner dielectric layer. Vieira *et al.* (2017), further showed improvements in the transport efficiency of the droplet by coating the PDMS with a chemical compound called Glaco®, which is mainly a perfluoroalkyltrichlorosilane combined with perfluoropolyether carboxylic acid and a fluorinated solvent (Kato *et al.*, 2008). Glaco®, improves the dynamic response of the droplet, turning the dielectric surface superhydrophobic (depicting equilibrium contact angles θ_e=153±2º, with a hysteresis lower than 10º, as measured by Vieira *et al.* 2017) and reducing the

adsorption of the biocomponents by the PDMS, which was shown to improve the local wettability at droplet-dielectric surface interaction. However, Vieira *et al.* (2017) also show that the Glaco® coating increases substantially the thickness of the dielectric layer, turning difficult for the droplet to respond to the electrical actuation, according to Young-Lippmann equation. Consequently, despite functional, the chips are working under very high imposed voltages and frequencies. Hence, to scale down the transport section, addressing smaller dimensions and thinner dielectric layers, a model was developed and simulations were performed using COMSOL Multiphysics 4.3b, as described in Section 2.2. It is worth reminding that the boundary conditions addressing the wettability of the dielectric surface were set to match the set PDMS+Glaco (θ_e = 153º) and the biofluid droplet has the properties depicted in Table 1 for GFP ($1.71x10^{-3}$m). The thickness of the film was reduced to 10µm, following the recommendations of Di Virgilio (2015) and of Mata *et al.* (2016). The first important output taken from the simulation performed was the electric force generated by the electric field, for different distances between electrodes 2*a*. The results, depicted in figure 5 show that the distance *2a* considered in the experimental approach was over dimensioned and that the optimum distance which maximizes the electric force generated is around 10µm. The values obtained for the electric force are in qualitative agreement with those reported by Di Virgilio (2015), with a similar geometry. Performing the entire simulation of the dynamic behaviour of the droplet for the optimum distance between electrodes *2a* = 10µm, as depicted in figure 6, the droplets shows a significant motion for an applied voltage of 70V, which is significantly lower than the 200V required in the first tested set of chips. Also, the imposed frequency could be lowered down to 9Hz, matching the very low values achieved by Fan *et al.* (2007). Overall the dynamic behaviour of the droplet is in qualitative agreement with that reported in the simulations of Di Virgilio (2015). The nearly independent dynamic response of the droplet with the imposed frequency, shown in the experimental tests is well patent in the simulation and in the results of Di Virgilio (2015): droplet motion is not affected even at frequencies lower than the 50Hz experimentally tested.

Despite preliminary, these results are quite promising, considering that other parameters such as the thickness of the dielectric layer can be further optimized. The new patch of chips being currently produced are following a fabrication method allowing a more precise control of the thickness of the dielectric layer, so that it can be quite reduced now. This new patch of chips will now be tested following a procedure similar to that reported here to then be integrated in the more complex design of the entire microdevice, towards the assembly of the final prototype.

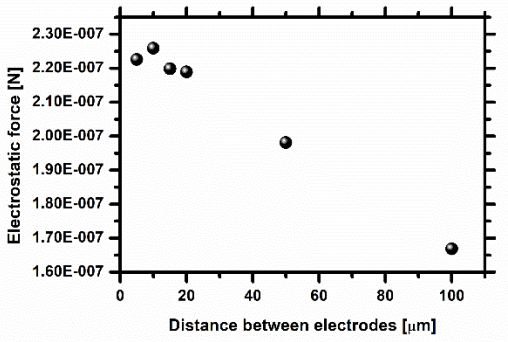

Figure 5: Electric force generated by the electrodes configuration, as a function of the distance between electrodes.

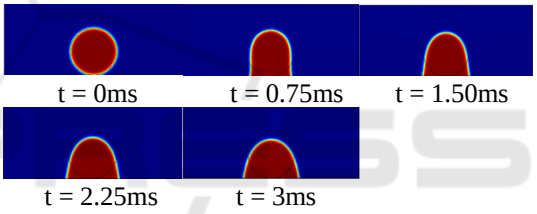

Figure 6: Sequence of images showing the motion of the GFP droplet on co-planar electrodes, spaced with a distance 2a = 10µm, for an imposed electric potential of 70V and an imposed frequency of 9Hz. The volume of the liquid droplet is 1.8µL.

4 CONCLUSIONS

The present paper describes the design, microfabrication and test of an electrowetting chip to transport and manipulate biosamples, towards the development of a microfluidic device for clinical diagnostics, based on cell elasto-mechanical properties and on the rheology of the biofluidic droplets. Emphasis is put here in the design of the section for sample manipulation and transport. Experiments are performed, at an earlier stage of the work, to determine basic chip dimensions and configuration (size and positioning of the electrodes), allowing its best performance, evaluated based on droplet dynamics (spreading/receding diameter and contact line velocity). Then, to scale down this section, for its proper integration in the

device, these basic dimensions serve as input for a numerical model, used to optimize the distance between the electrodes, the thickness of the dielectric and the electric potential and frequency to be applied.

Preliminary results are promising, predicting the satisfactory behaviour of a chip where the distance between electrodes could be optimized to 10μm, for a dielectric thickness of 10μm. Under these conditions, the chip can transport droplets of the order of 0.65mm diameter (thus allowing the manipulation of biological flows containing cells) for imposed voltages up to 70V and imposed frequencies as low as 9Hz. These values are significantly lower than those achieved in the preliminary design stages, which could reach imposed voltages of the order of 230V.

ACKNOWLEDGEMENTS

The authors are grateful to Fundação para a Ciência e a Tecnologia (FCT) for partially financing this research through the project UID/EEA/50009/2013, and for supporting F. Jacinto with a fellowship.

A.S. Moita also acknowledges the contribution of FCT for financing her contract through the IF 2015 recruitment program and for partially financing this research through the exploratory project associated to this contract.

Finally, the authors acknowledge the contribution of Prof. Susana Freitas and her team from INESC-MN for the microfabrication of the test chips.

REFERENCES

Chen, J. Z., Darhuber, A. A., Troian, S. M., Wagner, S., 2004. Capacitive sensing of droplets for microfluidic devices based on thermocapillary actuation, *Lab-on-a-Chip*, 4(5):473–480.

Cooney, C. G., Chen, C. Y., Emerling, M. R., Nadim, A., Sterling, J. D., 2006. Electrowetting droplet microfluidics on a single planar surface. *Microfluidics and Nanofluidics*, *2*(5):435–446.

Dance, A., 2017. The making of a medical microchip. *Nature*, 545:512-514.

Di Virgilio, V., 2015. Contactless electrowetting, PhD Thesis, Universitat Politècnica de Catalunya, Catalunya, Spain, 2015.

Fan, S.-K., Yang, H., Wang, T.-T., & Hsu, W., 2007. Asymmetric electrowetting--moving droplets by a square wave. *Lab-on-a-Chip*, 7(10):1330–1335.

Geng, Hongyao., Feng, J., Stabryl, L. M., Cho, S. K., 2017 Dielectroetting manipulation for digital microfluidics: creating, transporting, splitting, and merging droplets. *Lab-on-Chip*, 17:1060-1068.

Gosset, G.R., Tse, H.T.K., Lee, S.A., Ying, Y., Lidgren, A.G., Yang, O.O., Rao, J., Clark, A.T., Di Carlo, D., 2010. Hydrodynamic stretching of single cells for large population mechanical phenotyping, PNAS, 109(20):7630-7635.

Kato M, Tanaka A, Sasagawa M, Adachi H, 2008. Durable automotive windshield coating and the use thereof. US Patent, 8043421 B2.

Li, Y., Fu, Y. Q., Brodie, S. D., Alghane, M., Walton, A. J., 2012. Integrated microfluidics system using surface acoustic wave and electrowetting on dielectrics technology. *Biomicrofluidics*, 6:012812.

Manz, A., Widmers, H. M., Graber, N., 1990. Miniaturized total chemical analysis systems: A novel concept for chemical sensing, *Sensors and Actuators B: Chemical*, 1(1-6):244–248.

Mata F., Moita, A.S., Kumar, R., Cardoso, S., Prazeres D.M.F, Moreira, A.L.N., 2016. Effect of surface wettability on the spreading and displacement of biofluid drops in electrowetting. *Proceedings of ILASS – Europe 2016, 27th Annual Conference on Liquid Atomization and Spray Systems*, Sep. 2016, Brighton, UK 4-7 September 2016. ISBN 978-1-910172-09-4.

Moita, A. S., Laurência, C., Ramos, J.A., Prazeres, D. M. F., Moreira, A. L. N., 2016. Dynamics of droplets of biological fluids on smooth superhydrophobic surfaces under electrostatic actuation, *J. Bionic Eng.*, 13:220-234.

Mugele F, Baret J C., 2005. Electrowetting: From basics to applications. *Journal of Physics Condensed Matter*, 17:R705–R774.

Sen, P., Kim, C.-J. C., 2009. Capillary spreading dynamics of electrowetted sessile droplets in air. *Langmuir*, *25*(8):4302–4305.

Vieira, D. Mata, F., Moita, A.S., Moreira, A.L.N., 2017. Microfluidic Prototype of a Lab-on-Chip Device for Lung Cancer Diagnostics. *Proceedings of the 10th International Joint Conference on Biomedical Engineering Systems and Technologies - Volume 1: BIODEVICES*, 63-68, 2017, Porto, Portugal, 21-13 February 2017. DOI: 10.5220/0006252700630068, ISBN: 978-989-758-216-5.

Wheeler A R, Moon H, Kim C J, Loo J A, Garrell R L., 2004. Electrowetting-based microfluidics for analysis of peptides and proteins by matrix-assisted laser desorption/ionization mass spectrometry, *Analytical Chemistry*, 76:4833–4838.

Wyatt, C. N., Kim, C.-J., 2012. Droplet actuation by Electrowetting-on-Dielectric (EWOD): A review. *J. Adhesion Sci. Tech.*, 26:1747-1771.

Yoon, J Y, Garrell R L., 2003. Preventing biomolecular adsorption in electrowetting-based biofluidic chips, *Analytical Chemistry*, 75:5097–5102.